Selecting New Construction Road Sections for Urban Area with Hazard Source Based on Resilience

GAO Ming-xia, QI Ming-tao, MO Jun-wen

Abstract— **In this research, we introduce a resilience-focused framework designed to enhance the operational robustness of urban road networks that interact with potentially hazardous industrial enterprises. Employing network theory, we introduce a unique metric grounded in system reliability and network connectivity to gauge the resilience-driven performance of a road transportation network. Referred to as NIP in our paper, the development of this resilience-oriented metric systematically incorporates factors such as network topology, redundancy levels, structural reliability, and the distribution of hazard sources. This approach enables a standardized assessment of risk mitigation alternatives, aimed at fortifying the resilience of urban road networks. Additionally, we propose a decision-making methodology to identify optimal solutions from various alternatives, including new construction possibilities, offering opportunities to bolster network resilience by modifying its existing topology. We present a bi-objective model aiming to maximize the resilience metric value while minimizing capital investment, employing the Non-dominated Sorting Genetic Algorithm II (NSGA-II) for solution optimization. Finally, we validate the proposed method using the hazard source area of Lanzhou city as a representative example.**

Index Terms—**Urban area with hazard source, Selection of new construction sections, Resilience-based performance metric, Bi-objective optimization**

I. INTRODUCTION

The urban road network serves as a crucial underpinning for social and economic activities within cities. While China's road traffic infrastructure has made considerable progress, recurrent incidents such as natural disasters, chemical plant explosions, and traffic accidents present a significant hazard to the safety of the transportation system. In the event of an accident, the traffic network must not only cater to specific requirements like evacuation and rescue operations but also ensure the continued smooth functioning of social and economic activities in the aftermath of the disaster.

The shift from a "never" attitude to a "proactive" attitude in the face of accidents has drawn increasing attention to the resilience of transportation networks among scholars [1-3]. Current research on transportation system resilience primarily revolves around conceptual frameworks [3-5], measurement indicators [6-9], and optimization strategies [10-14]. Gonçalves and Ribeiro [3] proposed a comprehensive review framework for the resilience of urban transportation systems, encompassing concepts, characteristics, and methodologies. Zhang et al. [4] introduced a matrix method for assessing node and link resilience, analyzing changes in network resilience by examining characteristic shifts in nodes and links during failure states. Bruneau et al. [5] introduced the "resilience triangle" concept, quantifying system resilience through post-disaster facility functional characterization and the time required to return to normalcy. Ma Chaoqun et al. [6] evaluated network performance loss by constructing an effective path sub-map and passenger flow loss metric following station failures, considering spatial and temporal characteristics of passenger flow in urban rail transit networks. Cox et al. [7] measured resilience by calculating the gap between predicted and actual passenger travel change rates post-emergency, suggesting that incorporating alternative travel modes enhances transportation system resilience. Chen [8] defined the resilience metric as the ratio of the Origin-destination (O-D) demand met by the transportation system before and after a disaster, employing a stochastic mixed-integer planning model to quantify the recovery capability of the freight system. Minette et al. [9] used a random mean regression model to study subway system disturbance propagation, assessing resilience through passenger volume recovery speed. Lv Biao et al. [10] proposed a resilience metric based on network efficiency, considering link capacity degradation and recovery, and devised a method for identifying link importance. Ma Min et al. [11] introduced a resilience assessment method for urban rail transit systems based on the network performance response function. They developed a recovery optimization model aimed at maximizing network resilience. Zhang Jiefei et al. [12] utilized average network efficiency as the resilience metric, presenting a method to assess subway network resilience under various repair schemes. They explored the impact of different repair strategies on network recovery performance. Reza et al. [13] employed the ratio of total travel time before and after road network damage as the resilience metric. They established a stochastic planning model to optimize resilience design across three scenarios: earthquake, flood, and terrorist attack. Ye et al. [14] adopted the traffic network performance recovery rate as the resilience metric, proposing a sequential decision model for road section reconstruction to maximize system resilience

Manuscript received September 25, 2023; revised September 23, 2024.

This work was supported in part by the National Nature Science Foundation of China under Grant 72261026; 62262037.

GAO Ming-xia is a professor of the School of Traffic and Transportation of Lanzhou Jiaotong University, Lanzhou, China (e-mail: mxgao@mail.lzjtu.cn).

QI Ming-tao is a postgraduate student of the School of Traffic and Transportation of Lanzhou Jiaotong University, Lanzhou, China (e-mail: 278924198@qq.com).

MO Jung-wen is a professor of the School of Economics and Management of Lanzhou Jiaotong University, Lanzhou, China (e-mail: 360685714@qq.com).

within budget constraints. Zhang et al. [15] integrated network topology, redundancy, traffic flow, damage degree, and available resources into the stochastic process for post-disaster recovery strategy optimization. They put forth a scheduling method for optimizing the post-disaster recovery of bridge transportation networks.

Previous research on resilience optimization strategies primarily focused on the recovery sequence of damaged bridges or road sections post-disaster. However, it's worth noting that altering the existing topology of the road network, such as creating new links to connect previously isolated nodes, can also enhance the network's resilience and bolster its capacity to withstand disasters [16]. In certain heavily industrialized cities of China, where hazard source enterprises are densely concentrated due to historical factors, there is a heightened likelihood of disasters, coupled with insufficient reserve capacity in the road network. In light of this scenario, this paper explores an optimization approach for road expansion design in such areas, aiming to strengthen the overall resilience of the road network. Taking into account factors like road network structure and hazard locations, the paper introduces a metric for assessing road network resilience performance in hazard-prone areas, along with the corresponding calculation process for the resilience metric value. A bi-objective programming model is formulated for the expansion optimization of road networks in hazard-prone areas, with the objectives of maximizing resilience performance and minimizing costs. The model is solved using the Non-dominated Sorting Genetic Algorithm II (NSGA-II). To validate the proposed method, a case study is conducted using the typical hazard source area of Lanzhou, China.

II. Resilience-based Performance metric of Road Network

A. Definition of the Performance Metric

At its core, the primary objective of a transportation system is to facilitate the movement of demand from its source to the destination. The resilience of this system is evident in its capacity to persistently fulfill this purpose even in the face of disasters. When severe events occur, causing damage to multiple roads simultaneously, the required financial and human resources for disaster recovery may not be readily accessible. Hence, the presence of alternative paths, redundant between O-D pairs, proves vital during both the emergency response phase and the extended recovery period following a disaster. These alternative routes stand as a fundamental characteristic of resilient transport networks. Therefore, by extending the concept proposed by Zhang and Wang [16], the resilience performance metric of a road network is defined as the weighted average number of reliable Independent Paths (IPs) between any O-D pair, where IPs refer to paths without overlapping sections.

Introducing the terminology of graph theory, let $\boldsymbol{G} = (\boldsymbol{V}, \boldsymbol{A})$ represent the road network, where $\boldsymbol{V} = \{1, 2, ..., n\}$ is the set of nodes representing major road intersections, and $\boldsymbol{A} = \{1, 2, ..., m\}$ is the set of arcs (links) representing road sections. The network performance metric, denoted as $NIP(\boldsymbol{G})$ and defined earlier, can be expressed as follows:

$$NIP(G) = \sum_{i=1}^{n} w_i r_i \tag{1}$$

where w_i is the weighting factor applied to individual node ,$i \in V, \sum_{i=1}^{n} w_i = 1$, and ri is the average number of reliable IPs between node i and any other n-1 nodes in the network, as expressed in Equation (2):

$$r_i = \frac{1}{n-1} \sum_{j=1, j\neq i}^{n} \sum_{k=1}^{K_{ij}} w_k(i,j) \cdot R_k(i,j) \tag{2}$$

in which $K(i, j)$ is the total number of IPs between nodes i and j; $R_k(i, j)$ is the reliability of IP $P_k(i, j)$, the kth IP between node i and node j; $w_k(i, j)$ is the weighting factor applied to IP $P_k(i, j)$, and for all $K(i, j)$ IPs between nodes i and j, $\sum_{k=1}^{K_{ij}} w_k(i,j) = K_{ij}$ .Each IP, denoted as $P_k(i, j)$, typically comprises multiple road links connected sequentially. Let a represent an individual road link, and q_a denote the reliability of link a. Therefore, for a series comprising independent links, the reliability of the path $P_k(i, j)$ is calculated as the product of the reliabilities of all the road links included in $P_k(i, j)$:

$$R_k(i,j) = \prod_{\forall a \in p_k(i,j)} q_a \tag{3}$$

In regular, daily situations, the parameter q_a is assumed to have a value close to 1 (e.g., 0.99). However, in emergency situations, its value is to be calculated by combining the daily reliability (0.99) with the distance between the link and the hazard source, as per Equation (4):

$$q_a = 0.99 \frac{l_{aj^*}}{L_{ij^*}^{\max}} \tag{4}$$

Where l_{aj*} represents the shortest path length of link a to the hazard node j*, which can be expressed as the shortest length from its head node to j*, and L_{ij*}^{max} represents the maximum value of the path length of any node i to node j*. By combining Equations (1) and (2), the resilience-based performance metric for the road network, denoted as $NIP(G)$, is expressed as:

$$NIP(G) = \sum_{i=1}^{n} w_i \frac{1}{n-1} \sum_{j=1, j\neq i}^{n} \sum_{k=1}^{K_{ij}} w_k(i,j) \cdot R_k(i,j) \tag{5}$$

Equation (5) introduces two weighting factors, namely w_i and $w_k(i, j)$. The factor w_i pertains to nodes and is computed based on the degree of the nodes, as outlined in Equation (6).

$$w_i = \frac{d_i}{\sum_{j=1}^{n} d_j} \tag{6}$$

The additional weighting factor $w_k(i, j)$ in Equation (5) pertains to IPs and is dependent on both the length and capacity of the IP. The length of the IP, denoted as $p_k(i, j)$

and represented by $L_{p_k(i,j)}$, is equivalent to the cumulative length of the links it encompasses :

$$L_{p_k(i,j)} = \sum_{a \in p_k(i,j)} L_a \tag{7}$$

For simplicity, the path length is normalized to obtain the equivalent path length, expressed by $L'_{pk(i,j)}$, as Equation (8), where L_{max} (i, j) represents the length of the longest IP between nodes i and j:

$$L'_{p_k(i,j)} = \frac{L_{\max}(i,j)}{L_{p_k(i,j)} \cdot \sum_{k=1}^{K_{ij}} (L_{\max}(i,j) / L_{p_k(i,j)})} \times K_{ij} \tag{8}$$

The capacity of the IP p_k (i, j), denoted by $u_{p_k(i,j)}$, is expressed as the minimum capacity of the link included in it:

$$u_{p_k(i,j)} = \min[u_a / a \in p_k(i,j)] \tag{9}$$

The normalized capacity of the path p_k(i,j) is then defined as:

$$u'_{p_k(i,j)} = \frac{u_{p_k(i,j)}}{\sum_{k=1}^{K_{ij}} u_{p_k(i,j)}} \times K_{ij} \tag{10}$$

Combined with Equations (7) - (10), the weight w_k (i, j) of the path p_k (i, j) is calculated as follows:

$$w_k(i,j) = b \cdot L'_{p_k(i,j)} + (1-b) u'_{p_k(i,j)} \tag{11}$$

In which $b \in [0,1]$, and can be determined according to the specific situation of the urban area.

B.Calculation of the Performance Metric Value

The crucial step in computing *NIP*(***G***) is identifying IPs for all O-D pairs. The algorithm for locating these IPs is illustrated in Fig 1 and is based on Dijkstra's algorithm. Once all IPs are identified, the reliability $R_k(i, j)$ of each IP is computed using Equations (3) and (4) for each O-D pair. Subsequently, the weight $w_k(i, j)$ of each IP is determined sequentially using Equations (7) through (11). After processing all O-D pairs, the weights w_i for all nodes are calculated using Equation (6). Finally, the resilience metric value of the road network is computed in accordance with Equation (5).

III. Model and Algorithm

A. Model

In the context of a hazard source area in the city, the objective is to enhance the road network's performance by constructing new sections to connect previously unlinked intersections. However, financial constraints dictate that only certain sections can be chosen for new construction. Consequently, the model's goal is to maximize the network resilience performance while minimizing the associated construction cost. Consider a set of candidates represented by $\boldsymbol{S}=\{s_1,s_2,...,s_s\}$ and their corresponding costs as C={c1,c2,...,cs}. Let $x_t \in X, t = 1,2...s$ denote the decision variables, where t takes values from 1 to s.

$$x_t = \begin{cases} 1, & s_t \text{ is selected} \\ 0, & Otherwise \end{cases} \tag{12}$$

One of the objectives is to maximize the overall resilience performance of the road network, as follows:

$$Max \quad NIP(\boldsymbol{G}(\boldsymbol{X})) = \sum_{i=1}^{n} w_i(\boldsymbol{X}) r_i(\boldsymbol{X}) \tag{13}$$

G (***X***) represents the road network corresponding to decision ***X***, *NIP* (***G*** (***X***)) is the resilience metric of network ***G*** (***X***), w_i (***X***) is the weight of node i in network ***G***(***X***), and r_i(***X***) is the average number of reliable IPs between node i and other nodes in network ***G***(***X***).

Let $\theta(X)$ denote the cost associated with decision ***X***; the second objective function is to minimize the total cost:

$$Min \quad \theta(\boldsymbol{X}) = \sum_{t=1}^{s} c_t x_t \tag{14}$$

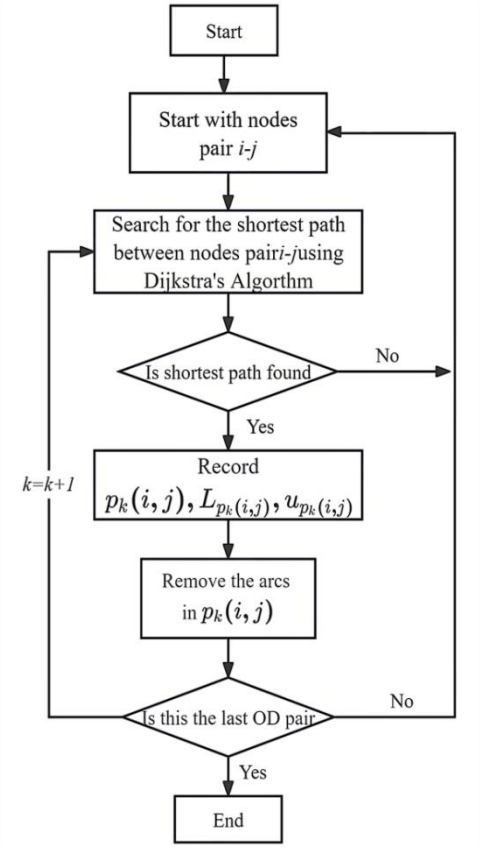

Fig 1. Calculation process of IPs between all O-D pairs in the network

B. Algorithm

Equations (13) and (14) present a challenging multi-objective optimization dilemma where a singular solution, optimizing both competing objectives—namely, maximizing *NIP*(***G***) and minimizing costs related to novel construction strategies—is unattainable. Instead, the scenario yields a set of Pareto-optimal solutions, allowing for a nuanced consideration of trade-offs between conflicting objectives and accommodating the subjective preferences of decision-makers in the decision-making process. The computation of the objective function in Equation (13) necessitates the application of the algorithm detailed in 1.2.1 and Figure 2. This involves a non-closed form formulation, prompting the use of metaheuristic

techniques to explore near-optimal solutions. Consequently, the NSGA-II [17] is employed to explore the Pareto Frontier. The NSGA-II has demonstrated success in seeking near-optimal solutions for analogous network problems [18-19], and specific algorithmic steps are omitted here. It is noted that preliminary parameter tuning involves setting the mutation parameter, crossover rate, and population size in the NSGA-II to 0.2, 0.65, and 100, respectively. The maximum number of iterations is capped at 900, and the early termination criterion is set at 50, implying that the program halts if no superior solution is identified in consecutive 60 iterations.

IV. Example

A. Example data

Using a local area within Lanzhou city as an illustration, Fig 2 delineates the area's extent, while the abstracted road network is portrayed in Fig 3. In Fig 3, numerical annotations alongside the sides indicate section length (unit: m) and capacity (unit: pcu/h). Nodes filled with shadows denote hazard sources, signifying proximity to a hazard source enterprise. Table I provides details on alternative section lengths and construction costs. In the context of urban development, dashed lines in Fig 3 represent links s_1-s_9, proposed as potential new constructions to mitigate risks. Assuming resources permit the construction of only three out of the nine candidates, specifically one section from (s_1, s_2, s_3), (s_4, s_5, s_6) and (s_7, s_8, s_9) respectively.

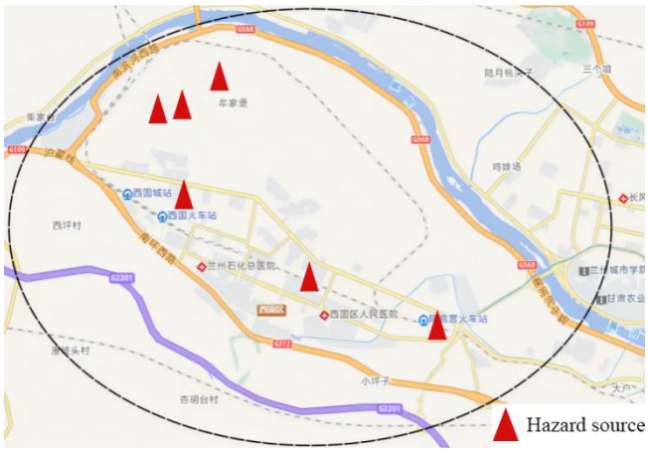

Fig 2. Area range and hazard source location

Table I. Length and cost of alternative links for new construction

Alternative links	Cost (ten thousand yuan)	Length (km)
s_1	9.8	1.4
s_2	4.2	0.6
s_3	9.1	1.3
s_4	7.0	1.0
s_5	3.6	0.5
s_6	2.6	0.4
s_7	2.1	0.3
s_8	2.8	0.4
s_9	4.5	0.6

B. Results

Table II lists the network resilience improvement and cost for the remaining schemes, excluding those with no discernible enhancement in network resilience.

In the event of an explosion at the hazard enterprise near node 48, varying levels of usage restrictions are anticipated on the adjacent roads. The reliability of each link is computed using the daily reliability factor (0.99) and the distance between the link and the hazard source, as per Equation (4). Subsequently, utilizing the updated link reliability, the road network resilience under each scheme in the disaster scenario is calculated, as illustrated in Table III.

Table II. Resilience and cost of each scheme in daily conditions

No.	Scheme	Resilience	Resilience improvement (%)	Cost (10 thousand yuan)
\	Original network	0.589	\	\
1	s_2+s_5+s_7	0.659	11.800	9.9
2	s_2+s_6+s_7	0.653	10.832	8.9
3	s_2+s_5+s_8	0.648	9.952	10.6
4	s_2+s_5+s_9	0.647	9.825	12.3
5	s_2+s_6+s_8	0.642	9.000	9.6
6	s_2+s_6+s_9	0.642	8.961	11.3

Table III. Resilience and cost of each scheme in the disaster scenario

No.	Scheme	Resilience	Resilience improvement (%)	Cost (10 thousand yuan)
\	Original network	0.071	\	\
1	s_1+s_4+s_7	0.101	42.253	18.9
2	s_3+s_4+s_7	0.095	33.803	18.2
3	s_1+s_4+s_8	0.088	23.944	19.6
4	s_1+s_5+s_7	0.081	14.085	15.5
5	s_3+s_4+s_8	0.074	4.225	18.9

A comparison between Table II and Table III reveals that the optimal scheme and outcomes differ between normal and disaster scenarios. Notably, in normal conditions, almost all resilience improvement schemes feature section s_2. However, when considering potential hazardous incidents near Node 48, none of the improvement schemes include section s_2, possibly due to its closer proximity to the hazard source. A similar pattern is observed in the selection set (s_4, s_5, s_6). Conversely, for the selection set (s_7, s_8, s_9), whether under normal or disaster scenarios, the schemes with greater resilience improvements consistently incorporate section s_7.

Fig 4 illustrates the comparison of resilience improvement (RI) and cost for each scheme under normal daily situations, while Fig 5 presents the comparison of RI and cost for each scheme in disaster scenarios.

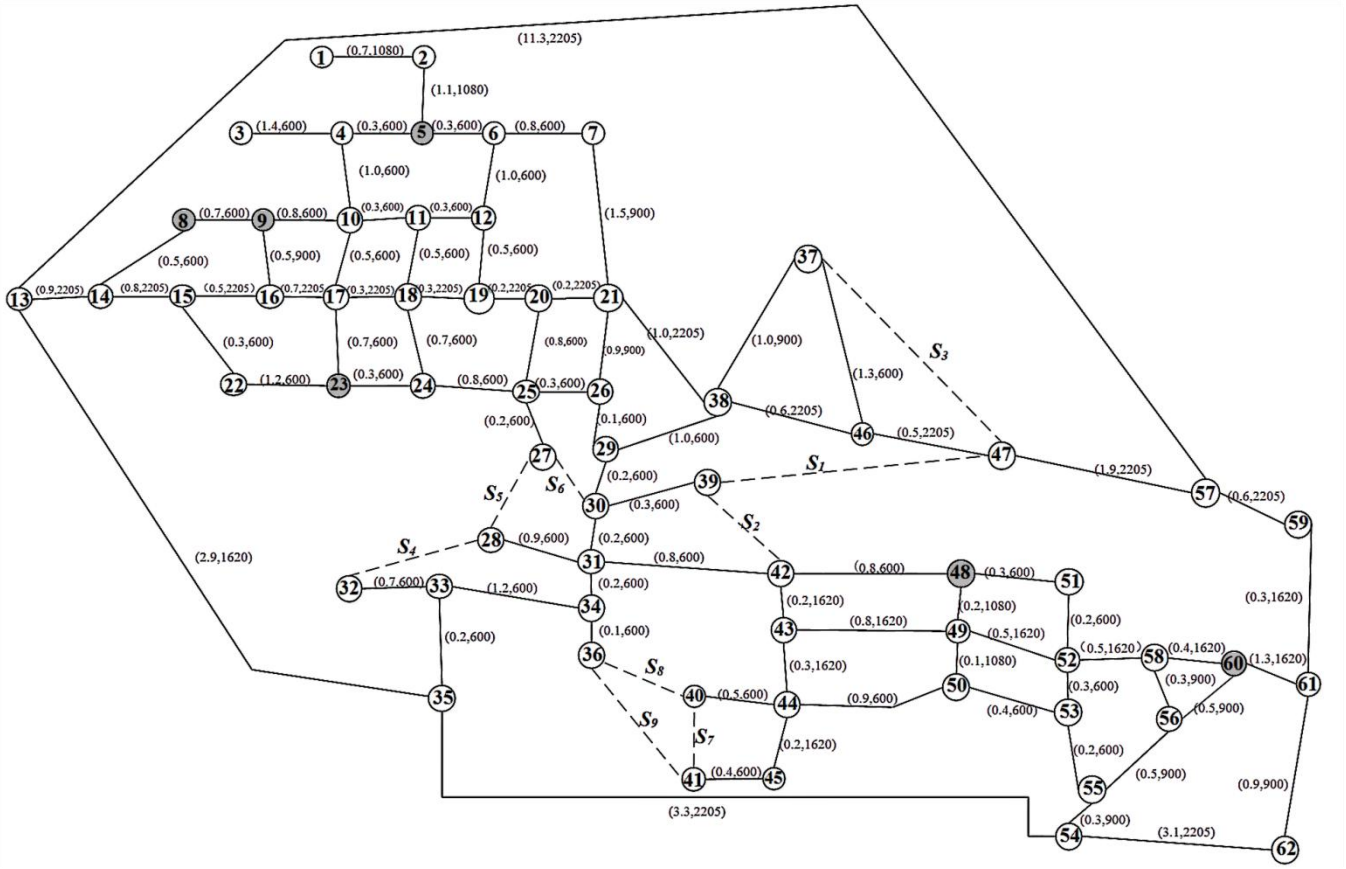

Fig 3. Abstracted network

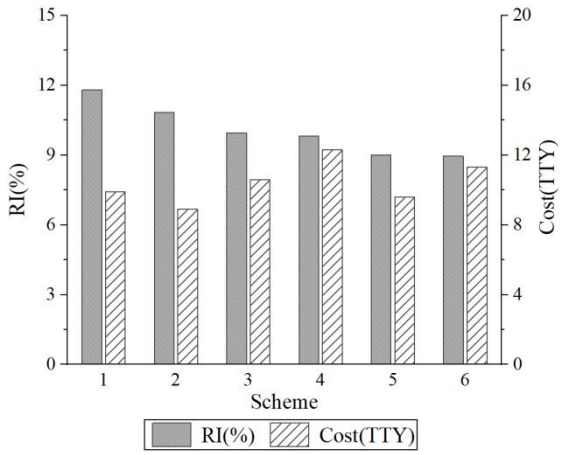

Fig 4. The resilience improvement and cost of each scheme in daily situations

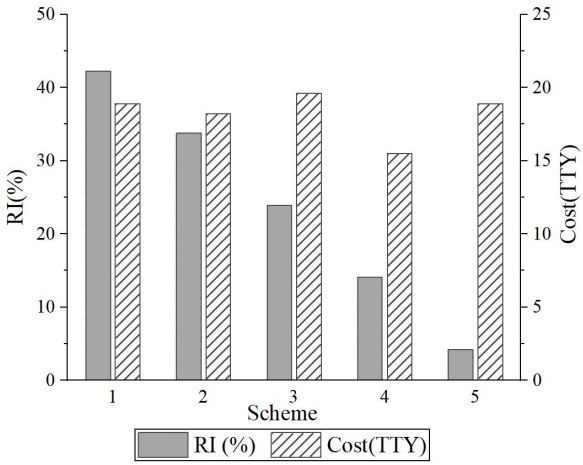

Fig 5. The resilience improvement and cost of each scheme in disaster scenarios

As depicted in Fig 4, there has been an enhancement in resilience, albeit not notably 12%.conspicuous in everyday scenarios, with a maximum range of less than Notably, Plan 1 exhibits the most substantial improvement in resilience at a comparatively lower cost (merely 10,000 yuan higher than the least expensive alternative, Scheme 2). Scheme 2, being the most cost-effective, marginally lags behind Plan 1 in resilience improvement. However, the remaining schemes exhibit shortcomings in both aspects. Examining Fig 5 reveals that certain disaster-oriented schemes significantly elevate road network resilience, reaching up to 40%. Nevertheless, the construction costs associated with these schemes are considerably higher. In either case, there is no perfect solution, and higher resilience consistently requires increased funding, especially in the face of disasters. Decision-makers are encouraged to select solutions based on their preferences and priorities in practical applications.

Additionally, calculations have been made for the global efficiency and average betweenness of the corresponding road networks under a number of schemes—metrics that are frequently used to evaluate the resilience of road networks[20–21]. Fig 6 illustrates the enhancements in these indicators for the six schemes under normal daily conditions. Conversely, Fig 7 presents the improvements in the indicators when factoring in the influence of disasters near Node 48.

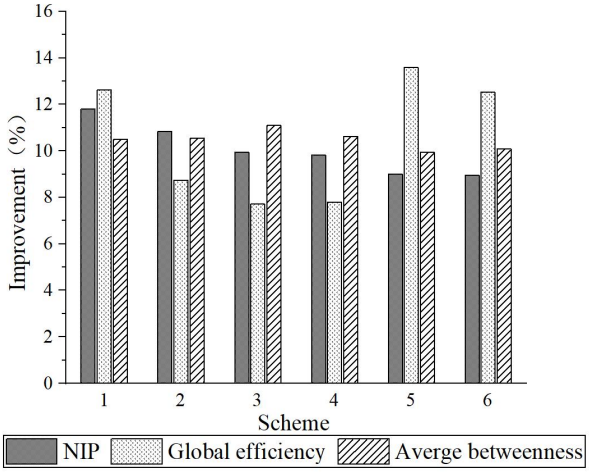

Fig 6. Improvement of resilience indicators by each scheme in daily situations

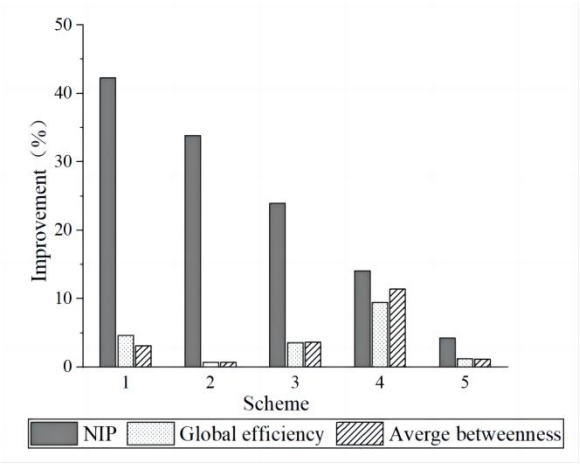

Fig 7. Improvement of resilience indicators by each scheme in disaster scenarios

The data presented in Fig 6 and Fig 7 indicates that, under normal (non-disaster) circumstances, a more substantial enhancement of NIP correlates with a notable improvement in the other two indicators. Contrastingly, during a disaster scenario, a scheme demonstrating significant improvement in NIP does not yield a satisfactory enhancement in the other two indicators. This discrepancy may stem from the fact that the calculation process for these two indicators requires the removal of Node 48, whereas the computation of NIP merely entails reducing the reliability of nearby sections.

C. Results verification

The road network may fail in parts due to accidents, disasters, and so on. The core definition of road network resilience is the network's ability to maintain good performance after road sections fail. Two typical indicators, size of largest connected subgraph (SLCS) and global efficiency (GE), are chosen to represent the performance of the road network, and the failure of road sections is simulated by attacking some edges in the network, so as to analyze the changes in the performance of the original network and the corresponding network of the optimal plan (optimized road network) after being attacked to different degrees. This approach verifies the results of resilience-based road network expansion optimization.

a. Results in daily scenarios

We select the road network under the optimal scheme, S2+S5+S7, for comparison with the initial road network. Fig. 8 shows the variation of SLCS between the two road networks, the optimized network and the initial network, depending on the attack ratio. The SLCS of the two road networks under typical attack ratios is shown in Table IV. The initial SLCS of both networks hovers around 60; when the attack ratio reaches 5%, the SLCS of the initial network drops to 35, and the optimized network shows no significant change; when the attack ratio reaches 10%, the optimized network begins to show a significant decrease; and when the attack ratio exceeds 20%, the SLCS of the two road networks shows little difference.

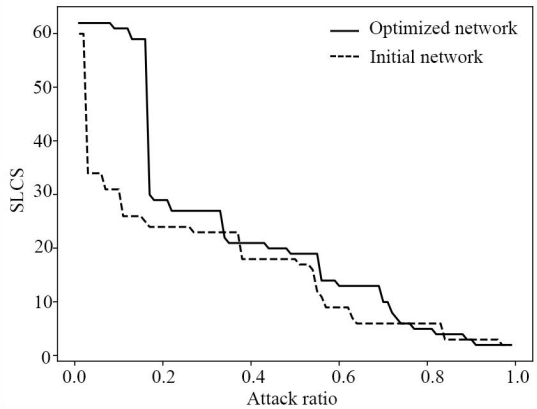

Fig 8. Variation of SLCS with attack ratio for two road networks in daily scenarios

Table IV. Typical attack ratios and their SLCS for two road networks in daily scenarios

Attack ratio	5%	10%	20%	35%	70%	90%
SLCS of initial network	35	26	24	23	6	3
SLCS of optimized network	61	60	28	23	12	3

Fig. 9 shows the variation in GE with attack ratio for both the optimized and original networks. The GEs of the two road networks with typical attack ratios are shown in Table V. When the attack ratio is less than 5%, the GE of the initial road network and the optimized road network are nearly the same; when the attack ratio is between 5% and 20%, the GE of the optimized road network is significantly higher than that of the initial road network; and there is not much difference between the GEs of the two road networks once the attack ratio exceeds 20%.

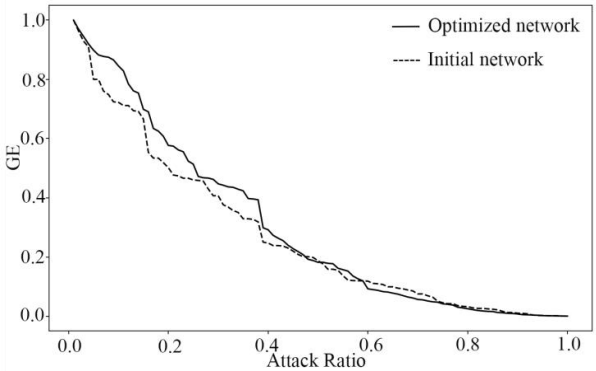

Fig 9. Variation of GE with attack ratio for two road networks in daily scenarios

Table V. Typical attack ratios and their GE for two road networks in daily scenarios

Attack ratio	5%	10%	20%	35%	70%	90%
GE of initial network	92%	73%	46%	35%	6%	0%
GE of optimized network	92%	86%	58%	43%	6%	0%

The results for both types of metrics show that the performance degradation of the optimized road network after an attack is lower than that of the original road network for most attack ratios.

b.Results in disaster scenarios

The optimal scheme for assessing the impact of disasters near node 48 is S1+S4+S7, and we select the optimized road network under this scheme for comparison with the initial road network. Fig. 10 shows the variation of SLCS between the two road networks, the optimized network and the initial network, depending on the attack ratio. Table VI shows the SLCS of the two road networks under typical attack ratios.

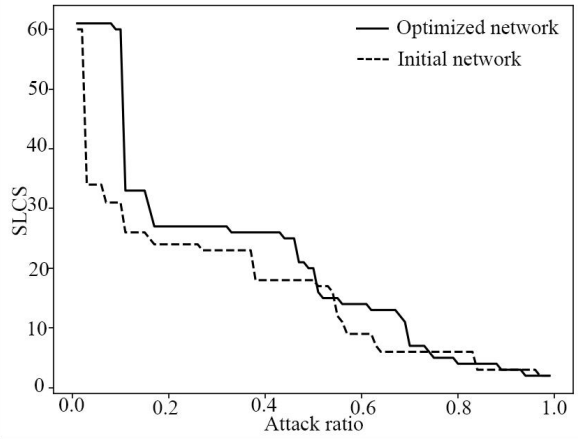

Fig 10. Variation of SLCS with attack rate for two road networks in disaster scenarios

Table VI. Typical attack ratios and their SLCS for two road networks in disaster scenarios

Attack ratio	5%	10%	20%	35%	70%	90%
SLCS of initial network	35	26	24	23	6	3
SLCS of optimized network	61	34	27	26	6	3

The SLCS of both road networks decreases more significantly when the attack percentage is between 5% and 10%; after the attack percentage is more than 20%, there is little difference between the SLCS of the two road networks. It is evident that the SLCS of the initial road network decreases significantly when the attack percentage reaches 5%, while the optimised road network shows no discernible change. Overall, the optimized road network's SLCS decline is less than that of the original road network.

Fig. 11 illustrates the variation in GE with attack ratio for both the optimized and original road networks under disaster scenarios. Table VII shows the GEs of the two road networks with typical attack ratios.

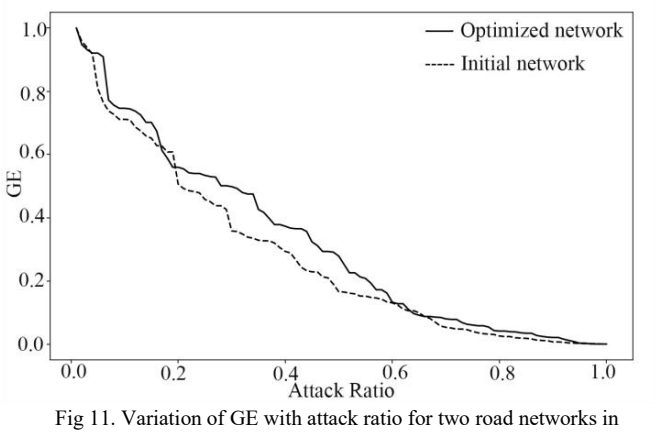

Fig 11. Variation of GE with attack ratio for two road networks in disaster scenarios

Table VII. Typical attack ratios and their GE for two road networks in disaster scenarios

Attack ratio	5%	10%	20%	35%	70%	90%
GE of initial network	82%	71%	48%	32%	5%	0%
GE of optimized network	92%	73%	54%	40%	8%	0%

When the attack ratio is between 10% and 20%, the GEs of both road networks decrease faster, but the optimized road network outperforms the initial road network by around 5%. When the attack ratio is between 20% and 60%, the global efficiency of the optimized road network significantly outperforms that of the initial road network, and the global efficiencies of the two networks converge to the same level after the attack ratio exceeds 60%. Overall, in the face of attacks, the optimized road network performs significantly better than the initial road network.

V. Conclusion

The study addresses the challenge of expanding road networks in densely populated urban areas with hazardous enterprises, focusing on enhancing overall resilience. The approach entails maximizing road network resilience with minimal capital investment by optimizing the selection of alternative new sections. The paper introduces a resilience performance metric and outlines a calculation process for its value. The paper establishes a bi-objective optimization model and solves it using the NSGA-II. To validate the method, we use a typical hazard source area of Lanzhou City as an example. The findings aim to offer insights into the expansion and construction of road networks in hazardous areas. We anticipate that the findings will provide valuable insights for designing and building the road network of hazard sources. This includes guidance on selecting the expansion or new sections that offer a substantial increase in resilience within the available fund constraints. Future research should explore the development of a resilience performance index that accurately reflects the road network's traffic flow state. Incorporating this index into the alternative optimization process is critical for increasing the rationality of optimization results.

References

[1] L-G Mattsson, E Jenelius. Vulnerability and resilience of transport systems-A discussion of recent research. *Transportation Research Part A: Policy and Practice*, vol. 81, pp. 16-34, 2015.

[2] C. Wan, Z. Yang, D. Zhang. Resilience in transportation systems: a systematic review and future directions. *Transport Review*, vol.38, no.4, pp. 1-20, 2017.

[3] L.A.P.J. Gonçalves, P.J.G. Ribeiro. Resilience of urban transportation systems: Concept, characteristics, and methods. *Journal of Transport Geography*, vol. 85, no. 1, Article ID 102727, 2020.

[4] C. Zhang, X. Xu, H. Dui. Resilience measure of network systems by node and edge indicators. *Reliability Engineering and System Safety*, vol. 202, no. 1, Article ID 107035, 2020.

[5] M. Bruneau, S-E. Chang, R-T.Eguchi. A framework to quantitatively assess and enhance the seismic resilience of communities. *Earthquake Spectra*, vol. 19, no. 4, pp. 733-752, 2003.

[6] C. Ma, S. Zhang, Q. Chen. Characteristics and vulnerability of rail transit network based on perspective of passenger flow characteristics. *Journal of Traffic and Transportation Engineering*, vol.20, no.5, pp.209-216, 2020.

[7] A. Cox, F. Prager, A. Rose. Transportation security and the role of resilience: A foundation for operational metrics. *Transportation Policy*, vol. 18, no. 2, pp. 307-317, 2011.

[8] L. Chen, M-H. Elise. Resilience: an indicator of recovery capability in intermodal freight transport. *Transportation Science*, vol. 46, no. 1, pp. 109-123, 2012.

[9] M. Lima, F. Medda. A new measure of resilience: An application to the London Underground. *Transportation Research Part A*, vol. 46, no. 1, pp. 35-46, 2015.
[10] B. Lv, Z-Q. Gao, Y-L. Liu.Evaluation of Road Transportation System Resilience and Link Importance. *Journal of Transportation Systems Engineering and Information Technology*, vol. 20, no. 2, pp. 114-121, 2020.
[11] M. Ma, D-W. Hul. Resilience assessment and recovery strategy on urban rail transit network. *Journal of Jilin University (Engineering and Technology Edition)*, vol. 53, no. 2, pp. 396-404, 2023.
[12] J-F. Zhang, G. Ren, J-F. Ma. Decision-making method of repair sequence for metro net-work based on resilience evaluation. *Journal of Transportation Systems Engineering and Information Technology*, vol. 20, no. 4, pp. 16-20, 2020.
[13] F. Reza, M-H. Elise. Travel time resilience of roadway networks under disaster. *Transportation Research Part B*, vol.70, no.1, pp.47-64, 2014.
[14] Q. Ye, V.U. Satish. Resilience as an Objective in the Optimal Reconstruction Sequence for Transportation Networks. *Journal of Transportation Safety & Security*, vol. 7, no. 1, pp. 91-105, 2015.
[15] W. Zhang, N. Wang, C. Nicholson. Resilience-based post-disaster recovery strategies for road-bridge networks. *Structure & Infrastructure Engineering*, vol. 13, no. 11, pp. 1404-1413, 2017.
[16] W. Zhang, N-Y. Wang. Resilience-based risk mitigation for road networks. *Structural Safety*, vol. 62, no. 1, pp. 57-65, 2016.
[17] K. Deb, A. Pratap, S. Agarwal, T Meyarivan. A fast and elitist multi-objective genetic algorithm: NSGA-II. *IEEE Trans Evol Comput,* vol. 6, no. 2, pp. 182-197, 2002.
[18] M-S Pishvaee, R-Z Farahani, W Dullaert. A. memetic algorithm for biobjective integrated forward reverse logistics network design. *Computers & Operations Research*,vol.37, no.6, pp. 1100-1112, 2010.
[19] I-H. Osman, J-P.Kelly. *Meta-heuristics: theory and applications.* Springer Science & Business Media, 2012.
[20] D-M. Zhang, F. Du, H. Huang et al. Resiliency Assessment of Urban Rail Transit Networks: Shagnhai Metro as an Example. *Safety Science,* vol. 106, pp. 230-243, 2018.
[21] A-C. Testa, M-N. Furtado, A. Alipour. Resilience of Coastal Transportation Networks Faced with Extreme Climate Events. *Transportation Research Record*, vol. 2532, no. 1, pp. 29-36, 2015.